University of Tsukuba Library

Free energy molecular dynamics simulations of pulsed-laser-irradiated SiO2: Si Si bond formation in a matrix of SiO2

Free energy molecular dynamics simulations of pulsed-laser-irradiated SiO₂: Si–Si bond formation in a matrix of SiO₂

Mauro Boero[a)] and Atsushi Oshiyama
Institute of Physics, University of Tsukuba, 1-1-1 Tennodai, Tsukuba, Ibaraki 305-8571, Japan

Pier Luigi Silvestrelli
INFM UdR Padova and DEMOCRITOS National Simulation Center, Trieste, Italy and Dip. di Fisica "G. Galilei," Università di Padova, via Marzolo 8, I-35131 Padova, Italy

Kouichi Murakami
Institute of Applied Physics, University of Tsukuba, 1-1-1 Tennodai, Tsukuba, Ibaraki 305-8573, Japan

Recent experiments have shown that pure Si structures in a matrix of SiO_2 can be formed by electron excitation techniques, with appealing applications in nanotechnology. Our *ab initio* simulations provide an insight into the underlying mechanism, showing that electron excitations weaken Si–O bonds in SiO_2, dislodge O atoms and allow Si dangling bonds to reconstruct in stable Si–Si structures *below the melting temperature*. Differences in diffusivity of O (fast) and Si (slow) are shown to play a decisive role in the process. © *2005 American Institute of Physics.*
[DOI: 10.1063/1.1929879]

Fabrication and fine control of Si nanostructures in a SiO_2 matrix is a basic requirement in the realization of Si-based nanodevices. Recent experiments have shown a new possibility to create Si nanocrystals in SiO_2 below the melting point of silica ($T_{melt}=1883$ K). Either immersing SiO_2 in a molten salt at 1123 K and injecting an electric current through a metal wire[1] or irradiating silica with femtosecond (fs) laser pulses[2,3] Si crystallization in SiO_2 has been evidenced. In the formation of Si nanostructures, the irradiated spots may be transformed to a liquid state (LS)[4] or to an excited solid state (ESS).[5,6] Then O atoms are expected to diffuse away from the irradiated areas so that seeds of Si crystals are formed. However, atom-scale processes are inaccessible experimentally and little is known about the mechanisms of the formation of Si seeds.

In this work, we perform free energy molecular dynamics (FEMD)[7] calculations,[8] allowing to simulate the dynamics of ions and electrons upon laser excitations[9,10] by controlling the electron temperature T_e: The excitation energy $\hbar\omega$ is distributed among electrons within fs, a time scale much shorter than the electron-ion relaxation time,[11] so that the adiabatic approximation holds. The calculations identifes the $\hbar\omega$ range at which either LS or ESS occurs and also how the diffusivities of O and Si differ upon high electron excitations. We find that in a certain range of T_e, though the ionic temperature T_I is much lower than T_{melt}, stable Si–Si bonds are formed. This clearly shows that the formation of Si nanocrystals is due to both the breaking of Si–O bonds upon electron excitation and to the different diffusion coefficients of Si (D_{Si}) and O (D_O). We also find that an oxygen vacancy, the most abundant defect in SiO_2, promotes the formation of the Si seeds.

The calculations are based on the density functional theory (DFT). The electron density $\rho(\mathbf{x})=\Sigma_i f_i|\psi_i(\mathbf{x})|^2$ is computed during the simulations by minimizing the free energy functional $\mathcal{F}=\Omega[\rho(\mathbf{x})]+\mu N_e+E_{II}$[7] where

$$\Omega[\rho(\mathbf{x})] = -2k_BT_e \ln \det[1+e^{-(H-\mu)/k_BT_e}] - \int d^3x\rho(\mathbf{x})$$
$$\times\left[\frac{V_H(\mathbf{x})}{2}+\frac{\delta E_{xc}}{\delta\rho(\mathbf{x})}\right]+E_{xc}, \quad (1)$$

H is the effective one-electron DFT Hamiltonian, V_H the Hartree potential, E_{xc} the exchange-correlation functional after Perdew *et al.*,[12] and E_{II} the ion–ion interaction. Occupation numbers are given by $f_i=[e^{(E_i-\mu)/k_BT_e}+1]^{-1}$ and valence wave functions are expanded in plane waves with a cutoff of 70 Ry with the Brillouin zone sampled at the Γ point. The core–valence interactions are described by Troullier–Martins pseudopotentials.[13] The system is a well assessed 24 formula units α-quartz supercell of $9.832\times8.514\times10.811$ Å^3 with experimental lattice parameters and periodic boudary conditions[14,15] [Fig. 1(a)]. We inspected $T_e=20\,000$, $25\,000$, and $30\,000$ K, corresponding to excitation energies $\hbar\omega$ of 1.72, 2.16, and 2.59 eV, respectively. However, these are not strictly related to the experimental excitations, due to the energy gap underestimation inherent in DFT.

Starting with a geometry-optimized SiO_2 system [Fig. 1(a)], we set $T_e=20\,000$ K and performed a FEMD for 1.2 ps. The ionic temperature T_I was found to equilibrate around 304 K (Fig. 2). However, no structural changes occurred, as clearly shown by the pair correlation functions (PCF) (Fig. 3).

In a second simulation at $T_e=25\,000$ K, the ionic forces $\nabla_{\mathbf{R}_I}\mathcal{F}$ change as a response to the enhanced T_e. After initial large oscillations, a new equilibrium is attained in about 1.9 ps with $T_I=367$ K, below T_{melt} (Fig. 2). Nevertheless, T_e is now sufficient to induce a weakening of several Si–O bonds, with large structural oscillations that in some cases result in a Si–O bond breaking. The longer equilibration time, in this case, reflects the structural modification, involving breaking and formation of chemical bonds and, although T_I is not too different from the former case, these chemical processes suppress or enhance T_I oscillations. Since it is easier for O to break its two bonds, rather than for Si to break
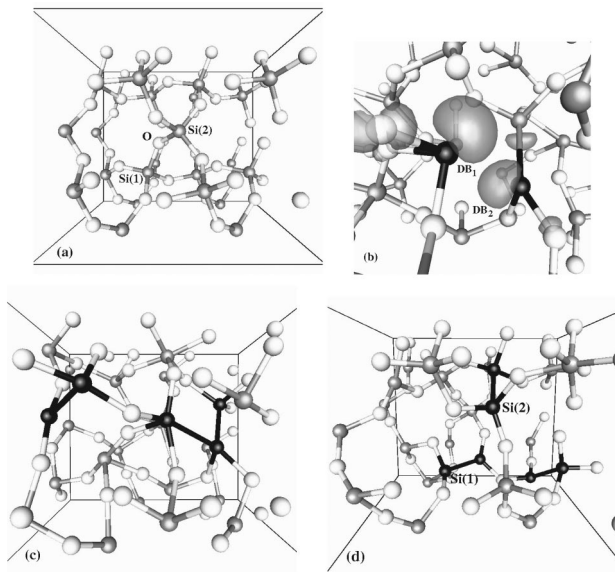
a)Electronic mail: boero@comas.frsc.tsukuba.ac.jp

FIG. 3. Si–O (upper panel) and Si–Si (lower panel) pair correlation functions (PCF) for $T_e = 20\,000$ K (dashed line), $25\,000$ K (solid line), and $30\,000$ K (dot–dashed line). The inset shows the details between 2.0 and 3.5 Å of the Si–Si PCF.

FIG. 1. (a) SiO_2 supercell: Si and O atoms are the gray and white balls, respectively; (b) detail of an intermediate configuration at $T_e = 25\,000$ K with two DB (DB$_1$, DB$_2$) ready to form a Si–Si bond (the two black Si). Isosurfaces (gray): $|\psi_i|^2 = 5 \times 10^{-3}$ Å^{-3}; (c) equilibrated SiO_2 structure at $T_e = 25\,000$ K (Si–Si bonds in black); (d) equilibrated ODC structure at $T_e = 25\,000$ K (Si–Si bonds in black).

all its four bonds, O atoms can be dislodged. This intuitive image is supported by the computed[16] diffusion coefficients[17] (Table I): D_O is more than twice larger than D_{Si}. Interestingly, the weakening of the Si–O bonds occurs in regions where the electron excitations localize. In fact, by monitoring the electronic structure, [Fig. 1(b)], we observed that, when an O atom diffuses away, it leaves behind two Si sp^3 DBs similar to E' centers in SiO_2.[3,14,15] These are located in energy at ~ 2.7–3.0 eV above the valence band of SiO_2, i.e., inside the SiO_2 gap, and are characterized by occupation numbers $f_i = 0.86$ and 0.82, respectively. These values are much larger than $f_i \lesssim 4 \times 10^{-2}$ corresponding to antibonding eigenvalues. Thus, the disruption of the bond network and the formation of Si Si bonds cannot be ascribed to a simple randomization caused by antibonding states occupation. Since the two DBs are close, a Si–Si dimer of average length 2.54 ± 0.08 Å is quickly formed and remains stable on the time scale of the simulation. The gap states corresponding to

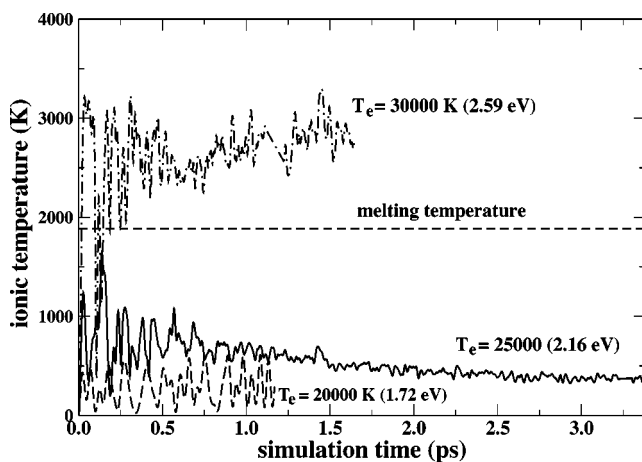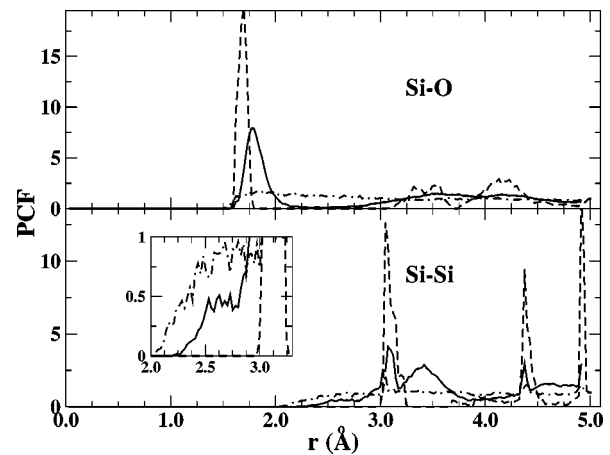the DBs disappear and the resulting electron wave functions is a typical Si–Si covalent bond. The final equilibrated structure is shown in Fig. 1(c). The total number of Si atoms forming stable Si–Si bonds, with lengths ranging from 2.51 to 2.64 Å, is $\sim 20\%$ of the total number of Si. This results in nonzero values around 2.6 Å of the Si–Si PCF (Fig. 3). The presence of $\equiv$Si–Si–O– structures is responsible for a shift toward 1.78 Å and a broadening of the first peak of the Si–O PCF. The broad peak at ~ 3.4 Å in Si–Si PCF, absent in other simulations at different T_e, originates from $\equiv$Si–Si–O–Si$\equiv$ and $\equiv$Si–Si–Si$\equiv$ structures. Interestingly, although $T_I < T_{melt}$, the formation of Si–Si structures occurs via lattice distortions promoted by the weakening of the chemical bonds and results in a *local* phase separation induced by electron excitations. Since we are working here in the μ-canonical ensemble, the departing O sits elsewhere and forms a three-membered ring[15] where a threefold O atom and a Si floating bonds (FB) coexist.

In our third simulation, at $T_e = 30\,000$ K, the ionic forces become so large that many Si–O bonds break and the system heats above T_{melt} in ~ 0.3 ps. The ions equilibrate at $T_I = 2870$ K (Fig. 2) and with a random distribution of Si and O atoms. The PCFs become almost structureless with only a signature of a dynamical short range order (Fig. 3). Bonds are continuously broken and reformed, lots of unbound atoms wander around and the energy gap is filled by a large population of unsaturated bonds. This is a typical LS of SiO_2, as confirmed by the enhancement of D_{Si} and D_O (Table I).

Finally, we inspected an oxygen deficient center (ODC) by removing the O atom in $\equiv$Si(1)–O–Si(2)$\equiv$ [see Fig. 1(a)]. For $T_e = 20\,000$ K, the two Si atoms facing the O vacancy form a Si–Si dimer of ~ 2.53 Å, as expected,[14] with no

FIG. 2. Ionic temperature evolution for the three electronic temperatures simulated.

TABLE I. Ionic temperatures (T_I) and O/Si diffusion coefficients (D_O, D_{Si}) for the simulated T_e. Error bars refer to dynamical oscillations of T_I.

T_e (K)	T_I (K)	D_{Si} (cm^2/s)	D_O (cm^2/s)
20 000	304 ± 118	1.00×10^{-9}	1.26×10^{-9}
25 000	367 ± 112	4.09×10^{-9}	8.49×10^{-9}
30 000	2870 ± 220	1.42×10^{-7}	3.40×10^{-7}

major modifications. On the contrary, when $T_e = 25\,000$ K Si(1) and Si(2) initially form a dimer that undergoes a very quick breaking. Si(2) moves beyond the plane of its neighbor O atoms forming a threefold O with a nearby oxygen site, while Si(1) carries an unpaired DB. This corresponds to a (meta)stable puckering configuration observed in ODCs.[14,15] From this point on, the evolution of the system follows a pathway similar to the case of the nondefective α-quartz, eventually stabilizing as in Fig. 1(d). In the whole system, four stable Si–Si bonds ($\sim 25\%$ of the total number of Si) with average distances ranging from 2.56 to 2.39 Å are formed in the regions where localized excitations induce a Si–O bond breaking and O diffusion. In the process, Si(1) loses its DB by forming a stable bond with one of the diffusing O atoms that, in turn, binds to another nearby Si. No DB survives, as seen by inspecting the electronic and atomic structures, but three-membered rings [e.g., close to Si(1) in Fig. 1(d)] and FBs arise. The amount of Si–Si bonds formed around an ODC (25%) is larger than in pristine SiO_2 (20%), suggesting that defects promote the formation of Si nanocrystals.

Summarizing, we provided a microscopic picture of the creation of Si–Si bonds in SiO_2 upon electron excitation, clarifying the issues of LS/ESS formation and Si/O diffusivities.

[1] T. Nohira, K. Yasuda, and Y. Ito, Nat. Mater. **2**, 397 (2003).

[2] K. Hirao, *Internal Modifications inside Glasses with a Femtosecond Pulse Laser*, Japan Soc. of Appl. Physics, 64th Autumn Meeting, Ext. Abstract 31p-F-6, 2003.

[3] N. Fukata, Y. Yamamoto, K. Murakami, M. Hase, and M. Kitajima, Appl. Phys. Lett. **83**, 3495 (2003).

[4] K. Murakami, H. C. Gerristen, H. van Brug, F. Bijkerk, F. W. Saris, and M. J. van der Wiel, Phys. Rev. Lett. **56**, 655 (1986).

[5] K. Sokolowski-Tinten, C. Blome, C. Dietrich, A. Tarasevitch, M. Horn von Hoegen, and D. von der Linde, Phys. Rev. Lett. **87**, 225701 (2001).

[6] L. Huang, J. P. Callan, E. N. Glezer, and E. Mazur, Phys. Rev. Lett. **80**, 185 (1998).

[7] A. Alavi, J. Kohanoff, M. Parrinello, and D. Frenkel, Phys. Rev. Lett. **73**, 2599 (1994).

[8] CPMD code by J. Hutter *et al.*, Max-Planck-Institut FKF and IBM Zurich Research Laboratory, 1995–2003.

[9] P. L. Silvestrelli, A. Alavi, M. Parrinello, and D. Frenkel, Phys. Rev. Lett. **77**, 3149 (1996).

[10] P. L. Silvestrelli and M. Parrinello, J. Appl. Phys. **83**, 2478 (1998).

[11] K. Seibert, G. C. Cho, W. Kütt, H. Kurz, D. H. Reitze, J. I. Dadap, H. Ahn, M. C. Downer, and A. Malvezzi, Phys. Rev. B **42**, 2842 (1990).

[12] J. P. Perdew, K. Burke, and M. Ernzerhof, Phys. Rev. Lett. **77**, 3865 (1996).

[13] N. Troullier and J. L. Martins, Phys. Rev. B **43**, 1993 (1991).

[14] M. Boero, A. Pasquarello, J. Sarnthein, and R. Car, Phys. Rev. Lett. **78**, 887 (1997).

[15] M. Boero, A. Oshiyama, and P. L. Silvestrelli, Phys. Rev. Lett. **91**, 206401 (2003).

[16] *Computer Simulation in Chemical Physics*, edited by M. P. Allen and D. J. Tildesley (Kluwer, Dordrecht, 1992).

[17] The O activation energy ($E_a = 1.36$ eV), estimated via Arrhenius plot, agrees with the experiment in: M. A. Lamkin, F. L. Riley, and R. J. Fordham, J. Eur. Ceram. Soc. **10**, 347 (1992).